Chapter 6
Terahertz Imaging System Based on Superconducting Heterodyne Integrated Receiver

R.V. Ozhegov, K.N. Gorshkov, Yu B. Vachtomin, K.V. Smirnov, M.I. Finkel, G.N. Goltsman, O.S. Kiselev, N.V. Kinev, L.V. Filippenko, and V.P. Koshelets

Abstract The development of terahertz imaging instruments for security systems is on the cutting edge of terahertz technology. We are developing a THz imaging system based on a superconducting integrated receiver (SIR). An SIR is a new type of heterodyne receiver based on an SIS mixer integrated with a flux-flow oscillator (FFO) and a harmonic mixer which is used for phase-locking the FFO. Employing an SIR in an imaging system means building an entirely new instrument with many advantages compared to traditional systems.

In this project we propose a prototype THz imaging system using an 1 pixel SIR and 2D scanner. At a local oscillator frequency of 500 GHz the best noise equivalent temperature difference (NETD) of the SIR is 10 mK at an integration time of 1 s and a detection bandwidth of 4 GHz. The scanner consists of two rotating flat mirrors placed in front of the antenna consisting of a spherical primary reflector and an aspherical secondary reflector. The diameter of the primary reflector is 0.3 m. The

R.V. Ozhegov • Y.B. Vachtomin • K.V. Smirnov
Moscow State Pedagogical University, 1 Malaya Pirogovskaya str., Moscow, Russia

CJSC "Superconducting nanotechnology", 5/22 Rossolimo str., Moscow, Russia

K.N. Gorshkov • M.I. Finkel
Moscow State Pedagogical University, 1 Malaya Pirogovskaya str., Moscow, Russia

G.N. Goltsman (✉)
Moscow State Pedagogical University, 1 Malaya Pirogovskaya str., Moscow, Russia

CJSC "Superconducting nanotechnology", 5/22 Rossolimo str., Moscow, Russia

National Research University Higher School of Economics, 20 Myasnitskaya Ulitsa, Moscow 101000, Russia
e-mail: goltsman@mspu-phys.ru

O.S. Kiselev • N.V. Kinev • L.V. Filippenko • V.P. Koshelets
Kotel'nikov Institute of Radio Engineering and Electronics, 125009 Moscow, Russia

operating frequency of the imaging system is 600 GHz, the frame rate is 0.1 FPS, the scanning area is 0.5×0.5 m^2, the image resolution is 50×50 pixels, the distance from an object to the scanner was 3 m. We have obtained THz images with a spatial resolution of 8 mm and a NETD of less than 2 K.

6.1   Introduction

Modern terahertz heterodyne receivers with ultimate sensitivity were developed primarily for astronomical missions as a part of big international projects. As a result, we have such instruments as the balloon-borne telescope TELIS, the plane-borne telescope SOFIA, the space-borne telescope HERSHEL, and a project of future space-borne telescope Millimetron. Recently there have been great advances in the development of both receivers and radiation sources of the terahertz range combined with a decrease of their prime cost so that these devices have become more accessible for a wide range of tasks.

Obtaining an image of an object is one of the most important tasks in the terahertz region. Such imaging systems can be used in many areas from medicine and security systems to navigation under poor visibility. However, this frequency region is rather difficult to work in owing to the so-called terahertz gap [1]: the power level of radiation sources falls off as one of approaches this region either from the radio or from the infrared frequencies. At the same time terahertz imaging systems have certain advantages over analogous systems operating at different frequencies. X-ray systems offer excellent spatial resolution of hidden objects but do not allow analysis of the composition of the object, and besides X-rays are potentially harmful to humans. IR systems provide good spatial resolution but most materials used in daily life are not transparent in the IR region. Radio frequencies have a good penetrating capability but its relatively low frequency does not afford good spatial resolution. Falling in the region between radio and IR waves, terahertz radiation has good penetrating capability and offers high spatial resolution, which makes it very attractive to security systems.

Terahertz imaging systems also allow performing spectral analysis of the substance of the object in hand [2] (see Fig. 6.1) and obtaining pictures of slices of this object with the use of mathematical processing [3] (see Fig. 6.2).

Passive systems receive thermal radiation of an object and thus an image is constructed. Such systems are called thermal imaging systems and require very sensitive receivers, which are usually direct detection receivers. Employment of a heterodyne receiver in a thermal imaging system allows one to use spectral information present in the thermal radiation of the object to deduce its chemical composition. This makes heterodyne systems attractive to medical and security systems. An example of a passive direct-detection imaging system based on antenna-coupled superconducting microbolometers technology is presented in [4].

Heterodyne systems employ either Schottky diode mixers [5], or superconductor-insulator-superconductor (SIS) mixers [6], or HEB mixers [7]. SIS mixers offer
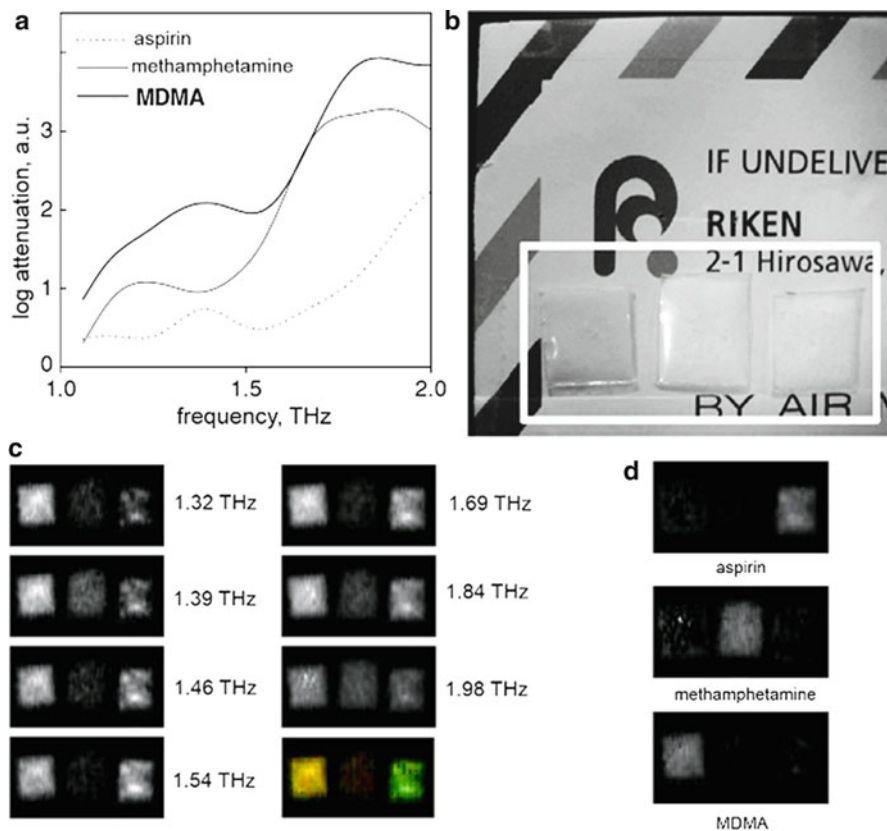
Fig. 6.1 Demonstration of capabilities of terahertz imaging systems to determine chemical composition of an object. (**a**) Spectral transmission lines of certain illegal drugs (MDMA, methamphetamine) and aspirin. (**b**) Observed objects, *left* to *right*: MDMA, aspirin, methamphetamine. (**c**) Terahertz images of objects taken at different frequencies. *Colour images* demonstrate possibility of detecting objects with the use of "colour" terahertz imaging. (**d**) Results of image processing [2]

low noise temperature and theoretically unlimited intermediate frequency (IF) bandwidth, but the RF range is limited by the properties of the superconductor. HEB mixers also offer a low noise temperature, but at frequencies below 1.3 THz SIS mixers have better noise performance. Schottky-diode mixers have worse noise performance than SIS and HEB mixers but do not require to be cooled down to the liquid He temperature. The noise performance of these three types of mixers is compared in Fig. 6.3.

Currently SIS mixers are the most sensitive heterodyne receivers in the frequency range 0.1–1.3 THz (see Fig. 6.3). Besides Josephson effects [8], one can observe in an SIS junction very strong nonlinearity of its current-voltage curve, which allows this junction to be used in a heterodyne receiver with a conversion gain and quantum-limited noise temperature. Superconducting junctions are also used
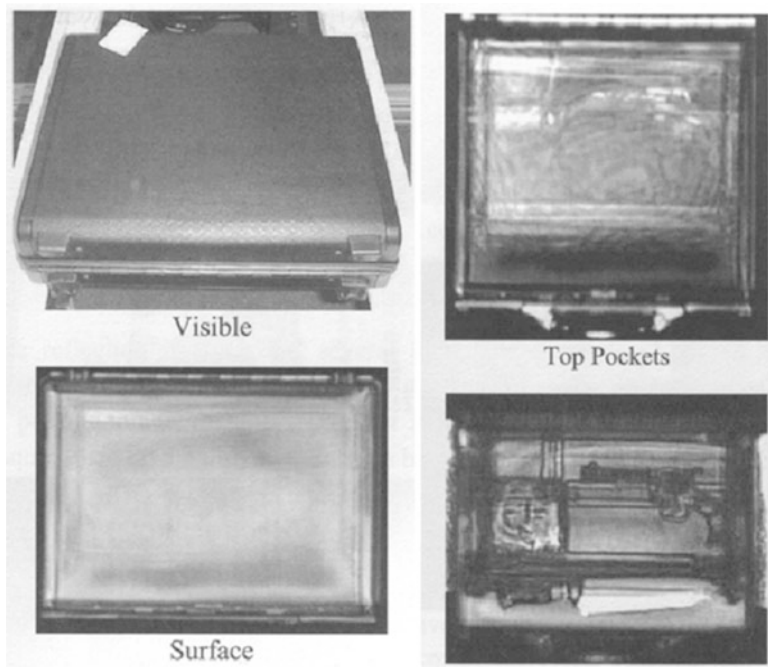
Fig. 6.2 An example of the performance of an active pulse imaging system receiving radiation reflected off the object [3]. By compensating the delay in the signal path it is possible to obtain images of various layers within the object. *Top left*: a photograph of the object (suitcase); *bottom left*: a terahertz image of the surface of the suitcase; *top right*: terahertz image of a plastic bag inside the suitcase; *bottom right*: terahertz image of the contents of the bag. One can clearly observe a knife and a gun inside the bag

as sources of high frequency current. An example of such a source is a flux flow oscillator (FFO) [9, 10].

Within the TELIS (TErahertz Limb Sounder) project, the research groups from the Institute of Radio Engineering and Electronics, the Russian Academy of Sciences (IREE), and the Space Research Organisation of the Netherlands (SRON) have built a superconducting integrated receiver (SIR)$4 \times 4 \times 0.5^3$ in size. The SIR carries an SIS mixer coupled with a planar quasioptical antenna and an FFO-based local oscillator (LO), and a harmonic mixer used to phase-lock the LO. The harmonic mixer technology is the same as that of the SIS mixer. A schematic of the SIR is presented in Fig. 6.4, and a photograph of the SIR chip is shown in Fig. 6.5. The SIR developed for TELIS [11, 12] has demonstrated successful performance under severe temperature, pressure and altitude conditions, and allowed collecting a lot of valuable information about the Earth's atmosphere. Despite the fact that the noise performance of SIRs is slightly worse compared to single SIS mixers, they become more and more attractive as candidates for compact spectrometers and imaging systems.
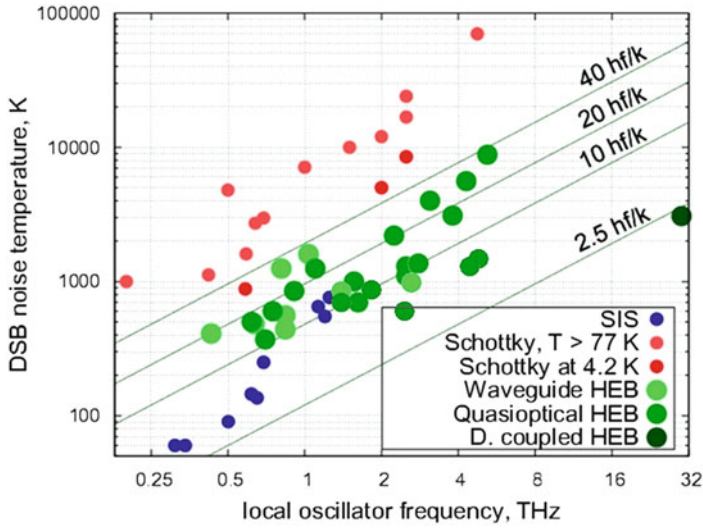
Fig. 6.3 Comparison of the noise performance of most widely used terahertz heterodyne receivers. For HEB receivers the data are given for both kinds of HEB mixers: waveguide and quasioptical ones
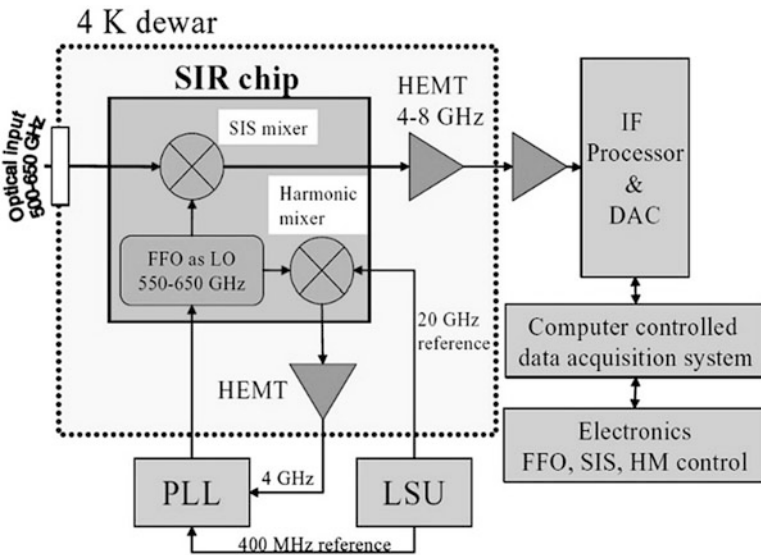
Fig. 6.4 A schematic of the SIR. To make the full use of the SIR one also needs a frequency synthesiser (LSU) and a PLL
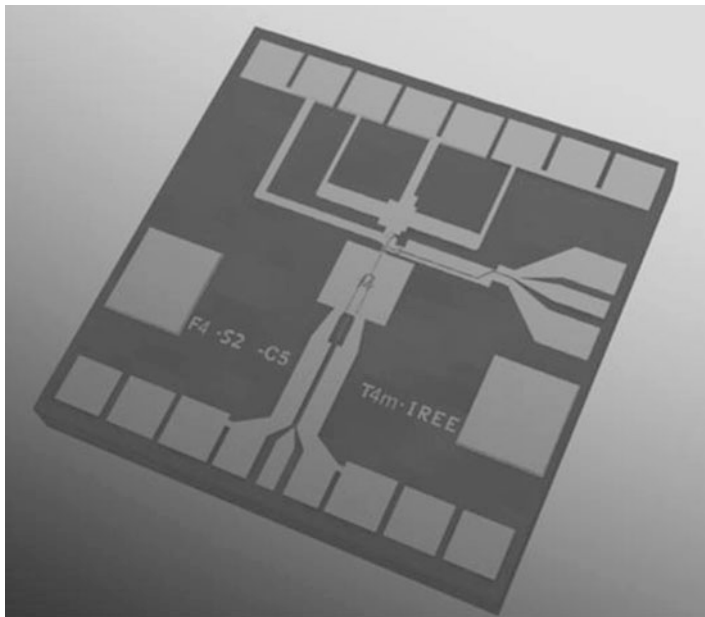
Fig. 6.5 A photograph of an SIR

Thus, one can put forward the requirements that a security system must meet in order to be economically efficient:

- capability of obtaining an image of an object which is up to 10 m away from the system;
- the system must be passive (this requirement is important in systems where the observer must not be seen and that monitor people, in which case the use of an active system is potentially harmful);
- capability of "seeing" objects hidden under clothing and in the luggage;
- capability of determining the material of the object;
- relatively low price of the ready-to-use system.

6.2   600 GHz SIR-Based Security System

The passive heterodyne thermal imaging system that we offer is currently unique. It potentially can be used for security purposes to detect plastic or metal weapon and explosives hidden under clothing, to check the post for illegal drugs, or in medicine to diagnose cancer at an early stage. The system has certain other advantages that makes it potentially the system of choice on the market of terahertz technology. The heart of the system is the SIR developed at IREE RAS. A series of tests of the SIR receiver performance was performed, and a model of an SIR-based imaging system was built without the phase-lock loop (PLL).

6.2.1 Receiver Performance

When an imaging system is used to obtain pictures of objects with temperatures of about 300 K, it may so happen that the system noise temperature will either be comparable with or less than the object temperature. In this case the system sensitivity is determined chiefly by the object temperature, and in the limiting case of a low-noise receiver the temperature resolution of the system is given by [13]:

$$\Delta T = 0.612\alpha \frac{T_S}{\sqrt{B_\tau}}. \tag{6.1}$$

In order to obtain the lowest possible temperature resolution we used a receiver with a large IF bandwidth, and also employed a PLL. The measurements were performed with the SIR T4m-093#6m offering a noise temperature of about 90 K at an LO frequency of 507 GHz. The main characteristics of this receiver are presented in Fig. 6.6.

We determined the temperature resolution of the receiver by measuring the rms voltage of the lock-in amplifier. Figure 6.7 shows time dependence of the lock-in read- out expressed in temperature units. As the magnitude of the input signal was lowered the temperature resolution improved. For the receiver T4m-093#6m looking at a temperature difference of about 173.5 K the temperature resolution was found to be 140 ± 15 mK; when the temperature difference was decreased to about 2.95 K, the temperature resolution reached 10 ± 1 mK. The error is determined by the integration time and is proportional to $(\tau/T)^{0.5}$, where τ is the time constant of the lock-in amplifier and T is the integration time.

Besides temperature resolution, another important parameter of a receiver operating as an imaging system is its temporal stability. In a system with a mechanical scanner, the time required to make one scan (frame time) can be a few seconds. This means that the time during which the system is considered stable (see below) must be much longer than the frame time, otherwise the temperature resolution of the system will be rather poor and the resulting image blurred.

To characterise the receiver stability one plots the so-called Allan variance as a function of the integration time [14]. The plot typically consists of three regions: the variance first decreases with time, then reaches a plateau, and finally increases as one makes the integration time longer. The Allan time is the integration time at which the Allan variance plot starts to depart from the $\sigma^2 \sim 1/\tau$ dependence.

In order to increase the Allan time one usually tries to achieve better temperature stability of amplifiers and bias sources. Alternatively, one can decrease the receiver input bandwidth [11].

The method of thermal stabilisation is rather challenging, expensive, and highly undesirable for mass production of receivers. The alternative method leads to degradation of the receiver sensitivity. That is why one has to look for different methods to improve the receiver stability. This is discussed below.

Various instabilities inherent in a receiver may manifest themselves either as fluctuations of the overall conversion gain, including the gain of the IF chain, or as fluctuations of the receiver noise temperature. As experience of working with HEB
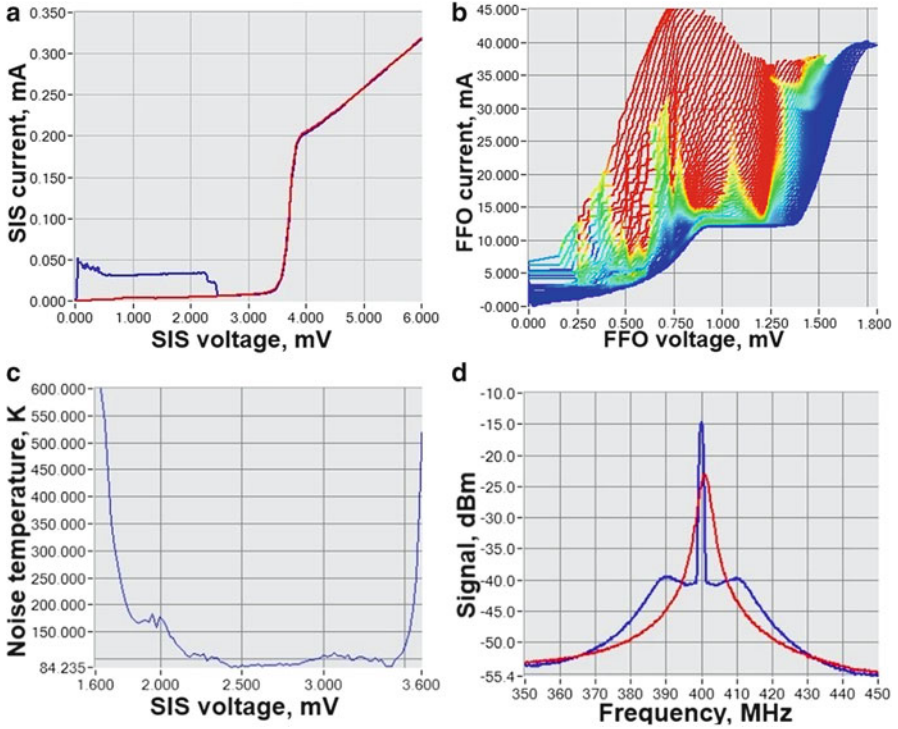
Fig. 6.6 The main characteristics of receiver T4m-093#6m. (**a**) Current-voltage characteristics (*CVC*) of the SIS mixer: the *blue* CVC corresponds to the unsuppressed DC Josephson effect; the *red* one corresponds to the optimal current of the control line suppressing the critical current of the tunnel junction. (**b**) CVCs of the FFO for different levels of magnetic field penetrating the junction; *colours* show the local oscillator (*LO*) drive level of the SIS mixer. (**c**) The receiver noise temperature as a function of the bias voltage. (**d**) The LO line with the PLL (*blue*) and without the PLL (*red*); the LO line is taken from the output port of the harmonic mixer integrated on the same chip with the SIS mixer at an IF of about 400 MHz

receivers of SIRs shows, gain fluctuations have a more dramatic effect on the system stability. That is why, as the first approximation, the receiver output is determined by the object brightness temperature and the instantaneous gain:

$$P_{OUT} = k_B \left(T_R + T_S \right) G B_H, \tag{6.2}$$

where k_B is the Boltzmann constant; B_H is operating frequency range; G is the total receiver IF gain, including the mixer conversion loss; T_R is the receiver noise temperature; T_S is the object brightness temperature.

To correct for gain fluctuations we used a wobbling mirror that could be switched between two positions: in one position the receiver was looking towards the reference load (77 K), in the other it was looking towards the signal load (300 K). The switching time was 1.8 ms [15].
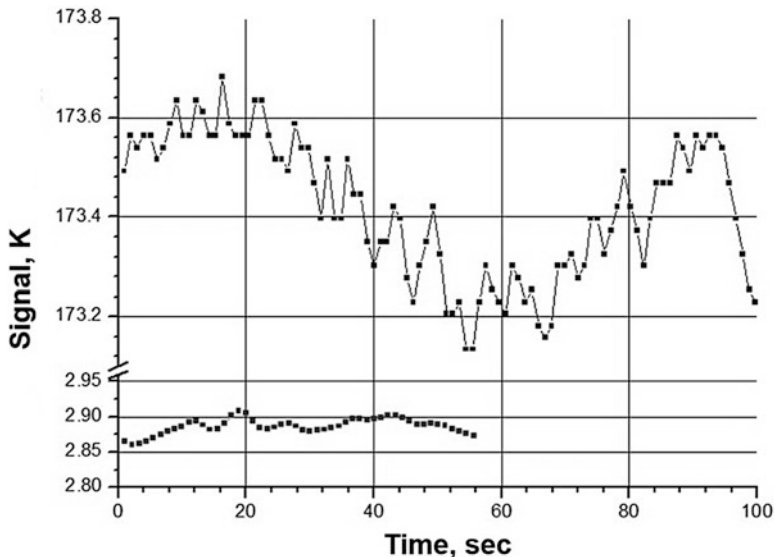
Fig. 6.7 Time dependence of the lock-in output for different levels of the receiver input signal for receiver T4m-093#6m. The input signal is the difference between the temperatures of the chopper blades and the load. In the case of a large difference (*top line*) NETD $= 143 \pm 14$ mK, and for a small difference (*bottom line*) NETD $= 10 \pm 1$ mK. In both cases the integration time of the lock-in amplifier was 1 s

The IF output was fed to the data acquisition system which also controlled the mirror and recorded its position. The data acquisition system computed the magnitude of the detected signals coming from the reference and source loads and adjusted them with the use of the expression:

$$S'_{OUT_i} = \frac{S_{OUT_i}}{S_{REF_i}} S_{REF_0}, \tag{6.3}$$

Here S_{REF_0} is the initial value of the output signal of the receiver looking towards the reference load; S_{OUT_i} and S_{REF_i} are instantaneous values of the output signal of the receiver looking towards the reference source load and reference load respectively, and S'_{OUT_i} is the corrected value of the output signal.

Figure 6.8 shows the Allan plots for the reference signal, the source signal, and the signal corrected according to 1.3. Fluctuations of the corrected signal at short integration times are shorter than fluctuation of each of the measured signals, in accordance with the expression $\sqrt{\sigma_{REF}^2 + \sigma_{OUT}^2}$. As can be seen from the plot, corrections allow one to reduce the contribution of the $1/f$ noise and drift noise by more than an order of magnitude, and increase the Allan time from fractions of a second up to 5 s, with an IF bandwidth of 4 GHz. The inset in Fig. 6.8 shows the result of correcting the output signal with a narrow IF bandwidth. In this case with
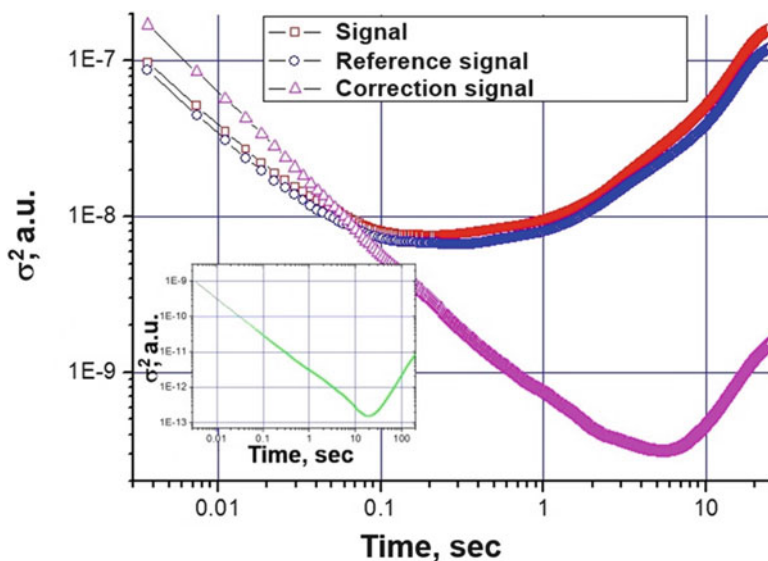
Fig. 6.8 The Allan plots for reference, source and corrected signals. The IF bandwidth is 4 GHz. The *inset* shows the corrected signal obtained with an IF bandwidth of 40 MHz

an IF bandwidth of 40 MHz it is possible to achieve an Allan time of 20 s. The data of the temperature resolution and the Allan time are unprecedented for heterodyne receivers of the terahertz range and are comparable with the best results obtained for direct detection receivers.
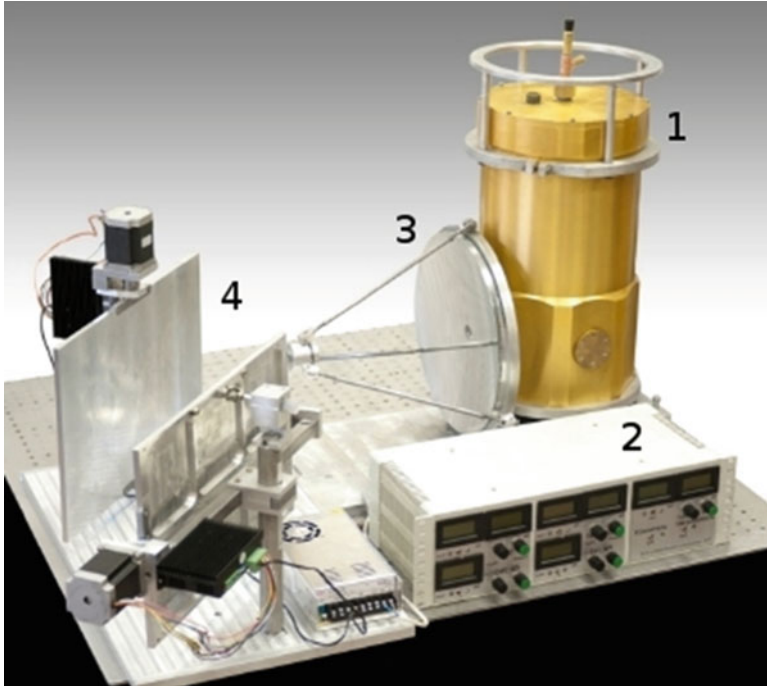
6.2.2 Model of the Imaging System

The imaging system consists of two main parts: SIR and front-end.

The SIR chip is glued onto a Si elliptic lens with an anti-reflection coating. The lens is installed into the mixer block mounted onto the cold plate of the He cryostat and enclosed with a cryomagnetic shield.

A photograph of the model of the terahertz imaging system is shown in Fig. 6.9. The front-end comprises a primary spherical dish 0.3 m in diameter with a secondary mirror 40 mm in diameter, and a mechanical scanner in front of the primary.

The scanner consists of two flat mirrors wobbling in mutually perpendicular directions. One is responsible for frame scans, the other for column scan. The sizes of the mirrors are 0.405×0.275 m^2 and 0.28×0.38 m^2, respectively. All the mirrors were made from a bulk piece of aluminium with the use of a milling machine. The mirrors are positioned with step motors. The scanning system allows performing observation of a relatively large spatial area. This however is possible at the expense of spatial resolution owing to decrease of the effective aperture. We

Fig. 6.9 A photograph of the model of the terahertz imaging system. *1* He cryostat with an SIR, *2* bias source of the SIR, *3* primary mirror, *4* mechanical scanner

achieved the following performance of system: time required to capture an image is 10 s, scanning area is 0.5×0.5 m^2, distance from the system to the object is 3 m, spatial resolution is better than 10 mm.

Some of the images taken with the model imaging system are presented in Fig. 6.10. The objects hidden under clothing were: a piece of chipboard 1 cm thick and measuring 10×3 cm^2 (top), and a packet of cigarettes in a breast pocket (bottom). The temperature resolution was less than 2 K.

6.3   Summary and Outlook

We have built a laboratory model of the terahertz imaging system with character-istics that will allow it to be developed into a commercial instrument for security applications. In order to develop such an instrument it is necessary to improve the scanner so that the frame time will be 1 s at most. This can be accomplished by replacing the step motors with more powerful AC servo motors, and by optimising the shape of the mirrors to reduce their moments of inertia. Replacing the He cryostat with a closed-cycle refrigerator will increase the system operation time
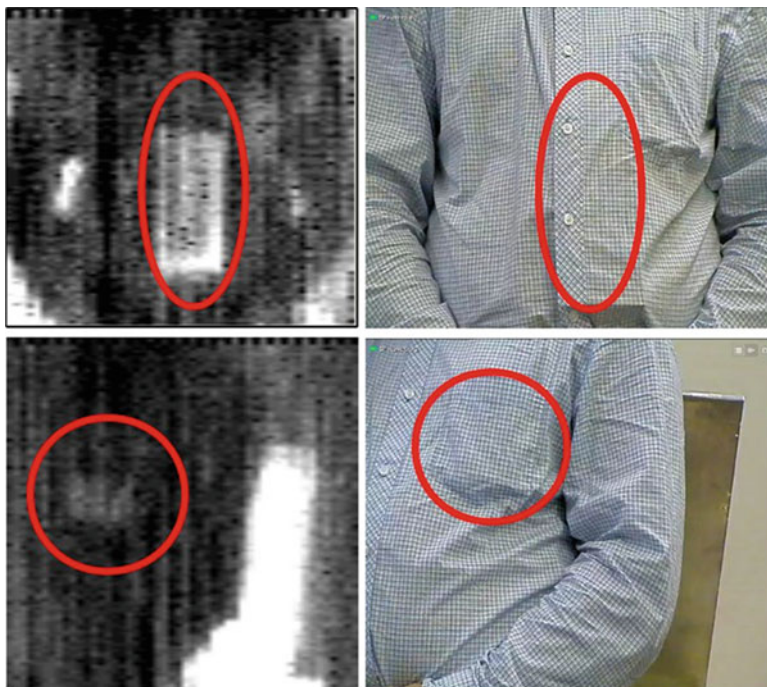
Fig. 6.10 Pictures taken with the model terahertz imaging system. *Left*: thermal images; *right*: optical images

by several orders of magnitude. Besides, it is necessary to improve the optics of the front-end of the system by adding elements that will allow switching between the object and the reference load. This will considerably improve the temperature resolution and stability of the system.

The passive heterodyne security imaging system has certain advantages over analogous active heterodyne and direct-detection systems, which will make it more attractive to the potential user.

References

1. Sisov F (2010) THz radiation sensors. Opto Electron Rev 18:10–36
2. Kodo Kawase, Yuichi Ogawa, Hiroaki Minamide, Hiromasa Ito (2005) Terahertz parametric sources and imaging applications. Semicond Sci Technol 20:258–265
3. Zimdars D, White J, Stuck G et al (2007) Time domain terahertz imaging of threats in luggage and personnel. Int J High Speed Electron Syst 17(2):271–281
4. Luukanen A, Gronberg L, Helisto P, Penttil JS, Seppa H, Sipola H, Dietlein CR, Grossman EN (2006) An array of antenna-coupled superconducting microbolometers for passive indoors real-time THz imaging. Proc SPIE 6212:270–27

5. Crowe TW, Mattauch RJ, Roser HP, Bishop WL, Peatman WCB, Liu X (1992) GaAs Schottky diodes for THz mixing applications. Proc IEEE 80:1827–1841
6. Richards PL et al (1979) Quasiparticle heterodyne mixing in SIS tunnel junctions. Appl Phys Lett 34:345–347
7. Gershenzon EM, Gol'tsman GN, Gogidze IG, Gousev YP, Elant'ev AI, Karasik BS, Semenov AD (1990) Millimeter and submillimeter range mixer based on electronic heating of superconducting films in the resistive state. Sov Phys Supercond 3:1582–1597
8. Josephson BD (1962) Possible new effects in superconducting tunneling. Phys Rev B 1:251
9. Nagatsuma T, Enpuku K, Irie F, Yoshida K (1983) Flux-flow type Josephson oscillator for millimeter and submillimeter wave region. J Appl Phys 54:3302. doi:10.1063/1.332443
10. Qin J, Enpuku K, Yoshida K (1988) Flux-flow-type Josephson oscillator for millimeter and submillimeter wave region. IV. Thin-film coupling. J Appl Phys 63:1130. doi:10.1063/1.340019
11. de Lange G, Boersma D, Dercksen J, Dmitriev P, Ermakov AB, Filippenko LV, Golstein H, Hoogeveen RWM, de Jong L, Khudchenko AV, Kinev NV, Kiselev OS, van Kuik B, de Lange A, Rantwijk J, Sobolev AS, Mikhail Y, Torgashin EV, Yagoubov PA, Koshelets VP (2010) Development and characterization of the superconducting integrated receiver channel of the TELIS atmospheric sounder. Supercond Sci Technol 23:45–61
12. Koshelets VP, Dmitriev PN, Ermakov AB, Filippenko LV, Khudchenko AV, Kinev NV, Kiselev OS, Sobolev AS, Torgashin MY (2009) On-board Integrated submm spectrometer for atmosphere monitoring and radio astronomy. ISTC thematic workshop on perspective materials, devices and structures for space applications, Yerevan, Armenia, 26–28 May
13. Esepkina NA, Korolkov DV, Pariyskiy YN (1973) Radiotelescopes and radiometers (in Russian)
14. Allan D (1966) Statistics of atomic frequency standards. Proc IEEE 54:221–230
15. Ozhegov RV, Gorshkov KN, Gol'tsman GN, Kinev NV, Koshelets VP (2011) Stability of terahertz receiver based on superconducting integrated receiver. Supercond Sci Technol 24:035–038